A Hybrid Empirical-Stochastic Method for Ground Motion Simulation; A Sample Study: The 22 February 2005 (MW 6.4) Zarand (Central Iran) Earthquake

H. Zafarani
International Institute of Earthquake Engineering and Seismology (IIEES), Tehran, Iran

SUMMARY:
Using the benefits of both stochastic finite-faults method and empirical Green's function method a simulation method has been developed which is very suitable for regions similar to the Iranian plateau. In this method the source spectrum comes from omega-square source model of finite-fault model and site and path effects comes from the deconvolved motion of small events. On 22 February 2005 at 02:25 GMT, a shallow destructive earthquake of Mw 6.4 occurred in Zarand region (central Iran). The proposed method for simulating strong ground motions from finite faults is applied to the records of this earthquake. The strong motion simulations are performed using model parameters based on the results of previous studies, and adjusting the sub-fault size and slip velocity to calibrate the simulation model against recorded ground motions. In conclusion, we found that the overall agreement between simulated and observed waveforms and spectra is quite striking. The method however, has the inherent limitation of needing the nonlinearity assumption.

Keywords: Strong motion Simulation, Empirical-Stochastic method, Empirical Green's function, Iran

1. INTRODUCTION

The strong motion simulation techniques are widely used in the engineering seismology and earthquake engineering. Simulation methods are the preferred approach for seismic hazard assessment in regions with moderate to low seismic activity where the latest event dates back to the pre-instrumental ear. Two main branches of simulation approaches, namely, empirical Green's function (e.g. Irikura, 1983; Frankel, 1995; Haddon, 1996; Kohrs-Sansorny et al., 2005) and stochastic finite-fault methods (e.g. Beresnev and Atkinson, 1997) have shortcomings that restrict their applicability in regions such as the Iranian plateau (Hartzell et al. 1999). Since records of small earthquakes used as empirical Green's functions inherently include propagation and site effects, uncertainties associated with the crustal structure and local geology are eliminated (Hartzell, 1978&1992). However, in some of the applications of the empirical Green's function method, a detailed description of the source rupture process is required while some of these parameters are poorly constrained. Therefore, for practical simulation purposes, a more appealing approach is one in which a detailed description of the source process of a future earthquake is not required (Ordaz et al. 1995).

On the other hand, the stochastic finite-fault methods require a detailed knowledge of the path and site effects but less information about the source process. Incorporation of site amplification effects in this method is usually one of the most troublesome tasks, because site-specific geotechnical information is usually limited or nonexistent. To overcome these limitations, here a hybrid Empirical-Stochastic method has been proposed for ground motion simulation which has the advantages of both empirical Green's function and stochastic finite-fault methods while avoiding their limitations. We test this method on a dataset produced by an M6.5 earthquake (22 February 2005), which occurred in the East-Central region of Iran, and its M 5.2 aftershock, whose recordings are used as empirical Green's functions. The synthesized records have been compared with the observed time histories of the larger earthquake to show the applicability and usefulness of the proposed technique.

2. METHOD

Let's assume a finite-fault plane discretized into equal rectangular elements, each of which is treated as a point source (named also as subfaults). The rupture spreads radially from the hypocenter. Seismic ground motions have been often modelled as a convolution of source, path propagation and local site effect factors. The total Fourier amplitude spectrum of the observed motion of the main shock $O_{ij}(f)$ can be expressed as a product of the source effect $S_{ij}(f)$, propagation path effect $P_{ij}(f)$, and site amplification effect $G(f)$ assuming linear systems (Boore, 1983)

$$O_{ij}(f) = S_{ij}(f) \cdot P_{ij}(f) \cdot G(f) \tag{2.1}$$

where ij refers to the sub-source number. Similarly the observed motion of aftershock $o_{ij}(f)$ at the same site can be expressed as:

$$o(f) = s(f) \cdot p(f) \cdot g(f) \tag{2.2}$$

Since we have discarded nonlinear wave propagation through the soil, it is reasonable to assume similar site effects for both main and aftershock motions

$$G(f) \approx g(f)$$

The source terms are represented by

$$S_{ij}(f) = C \cdot K_{ij}(f) \tag{2.3}$$

$$s(f) = C \cdot k(f) = C \cdot \frac{m_0}{1 + (\frac{f}{f_{ca}})^2}, \tag{2.4}$$

where

$$C = R^{\varphi\theta} \cdot \frac{FV}{4\pi\rho\beta^3} \tag{2.5}$$

where $R^{\varphi\theta}$ is the shear-wave radiation pattern, $V = 1/\sqrt{2}$ takes into account the partition of the total shear-wave energy into two horizontal components, F= 2 is the effect of the free surface, ρ and β are the density and shear-wave velocity in the vicinity of the earthquake source. As it is clear, we have assumed single-corner omega-square point source model (Brune, 1970&1971) for the aftershock. For subfault spectrums (i.e. $K_{ij}(f)$), Beresnev and Atkinson's (1997) source scaling of the omega-square spectrum has been used here (see below).

The path term was calculated by multiplying a simple geometrical spreading function $1/r_{ij}$ by a crustal attenuation term

$$P_{ij}(f) = \frac{1}{r_{ij}} P_{Pij}(f), \tag{2.6}$$

r_{ij} is the hypocentral distance of the source *ij* from the site. Similarly, for the aftershock we write as follow

$$p(f) = \frac{1}{r} p_P(f), \tag{2.7}$$

Here, r is the hypocentral distance of aftershock. We can assume that crustal attenuation is the same for both main and aftershock (Miyake et al. 2003)

$$P_{Pij}(f) \approx p_P(f), \tag{2.8}$$

Putting these relations in Eqn 2.1 results to

$$\begin{aligned} O_{ij}(f) &= \frac{r}{r_{ij}} \cdot S_{ij}(f) \cdot \frac{p(f) \cdot g(f) \cdot s(f)}{s(f)} \\ &= \frac{r}{r_{ij}} \cdot S_{ij}(f) \cdot \frac{o(f)}{s(f)} = \frac{r}{r_{ij}} \cdot K_{ij}(f) \cdot \frac{o(f)}{k(f)} \end{aligned} \tag{2.9}$$

Here, we have implicitly assumed the similarity of focal mechanism for main and aftershock (see Plicka and Zahradnik, 2002; Hartzell, 1992) which allows discarding the C factor. If we put $\frac{o(f)}{k(f)} = o'(f)$ then,

$$\begin{aligned} O_{ij}(f) &= \frac{r}{r_{ij}} \cdot K_{ij}(f) \cdot \frac{o(f)}{k(f)} \\ &= \frac{r}{r_{ij}} \cdot K_{ij}(f) \cdot o'(f) \end{aligned} \tag{2.10}$$

Taking the invers Fourier transform with the amplitude equal to Eqn 2.1 and phase of aftershock time series we have

$$O_{ij}(t) = \frac{r}{r_{ij}} \cdot K_{ij}(t) * o'(t) \tag{2.11}$$

Where $*$ denotes the convolution operator. Stochastic acceleration time histories are generated from each subfault using the method of Boore (1983), assuming an underlying omega-square spectrum which is multiplied by the normalized spectrum of a limited-duration Gaussian noise sample in order to produce a subfault spectrum that has a stochastic character. Here, Beresnev and Atkinson's (1997) source scaling of the omega-square spectrum has been used for $K_{ij}(f)$. In the stochastic model of Beresnev and Atkinson's (1997), the amplitude of the radiation at frequencies higher than the corner frequency of the subfaults is controlled by the radiation-strength factor s, and s parameter is related to the maximum slip velocity on the fault (Beresnev and Atkinson, 2002). Acceptable range for the values of sfact is 0.7–2.0. The presence of sfact allows us to calibrate the model more precisely. Also, it is possible to generate the range of desired scenarios taking into account the acceptable range of sfact parameter.

Finally, the ground motions of subfualts, each of which is calculated by the above mentioned procedure, are summed with a proper time delay in the time domain to obtain the ground motion acceleration, a(t), from the entire fault,

$$a(t) = \sum_{i=1}^{nl} \sum_{j=1}^{nw} O_{ij}(t + \Delta t_{ij}) \tag{2.12}$$

Here, Δt_{ij} is the proper time delay for subfault *ij*, nl and nw are number of subfaults along strike and dip, respectively. The time delay is the sum of three terms,

$$\Delta t_{ij} = r_{ij} / \beta + \xi_{ij} / Vr + \eta \tag{2.13}$$

Where, ξ_{ij} is the distance from the rupture nucleation point to subfault *ij*, Vr is the rupture velocity and η is a random number (see Beresnev and Atkinson (1997) for more details). The main idea is that taking into account the success of the stochastic finite-fault method in the representation of source term with a simple scheme, the deficiencies/uncertainties arise from the unknown path and site terms could be removed by using deconvolved empirical Green's functions.

3. SIMULATION OF ZARAND EARTHQUAKE

In order to investigate the applicability and efficiency of the proposed method, here we try to synthesize the records of a real earthquake occurred in the Iranian plateau. On 22 February 2005 at 02:25 GMT, a shallow destructive earthquake of Mw 6.4 occurred east of Zarand town (central Iran), about 60 km north of the city of Kerman, the provincial capital. The earthquake demolished much of the town and other neighbouring villages. Number of victims reached more than 600 people. Many of the structures in the region were poorly designed mud-brick constructions that collapsed quickly on sleeping inhabitants. The focal mechanism solutions as well as field observation show that this earthquake involved thrust faulting on a plane striking nearly east-west and dipping towards the north (Talebian et al., 2006). Twenty seven strong-motion instruments (SSA-2 accelerometers) of the BHRC located mainly within the state of Kerman recorded the mainshock.

The availability of these data, as well as the sufficient knowledge of the geometry of the causative fault, also destructiveness of this event was the most important motivation for simulating these acceleration waveforms. According to Talebian et al. (2006), the 2005 Zarand earthquake involved reverse faulting, unlike the strike-slip faulting responsible for the earlier recent earthquakes in this zone. It had a northward dip of about 67°, which is steep even for reverse faults (Talebian et al, 2006).

All of the available records were taken from the BHRC Database. Four strong motion stations recorded the main shock and a large aftershock (see Table 1&2). We selected records from stations located on free-field sites with clear P- and S-wave arrivals and a signal-to-noise ratio greater than 3. Table 3.1 lists the coordinates and site characteristics of these stations. The largest aftershock which has a similar focal mechanism like that the main shock has been selected as empirical Green's function. The Miyake et al. (2003) algorithm has been used for determination of corner frequency and moment magnitude of the aftershock. This method derives these parameters by fitting the observed source spectral ratio between the large and small events to the theoretical source spectral ratio, which obeys the omega-squared source model. The results are tabulated in Table 3.2.

Table 3.1. Recording characteristics of the strong-motion stations used

Code	Station Name	Lat. (degree)	Long. (degree)	Epicentral Distance (km)	Site class	PGA/L (cm/s/s)	PGA/T (cm/s/s)
CHT	Chatrood	30.60	56.91	28	hard rock	55	87
QAD	Qadrooni	30.96	56.82	19	rock	212	142
SHI	Shirinrood	30.81	57.03	28	stiff soil	500	196
ZAR	Zarand	30.81	56.57	16	soil	308	244

Table 3.2. Source parameters of the mainshock and aftershocks used in the current study.

Date	Lat. (degree)	Long. (degree)	Moment (dyne-cm)	Mw	Corner Freq.‡ (Hz)	Dip/Strike (degree)	Depth (km)
*2005/5/1	30.800†	57.000†	5.84e23	5.1	0.60	63/214	20.5 (14.1†)
2005/2/22	30.804	56.734	4.80e25	6.4	0.2	67/270	10.0

† From IIEES Web site; The other data for 2005/5/1 event is taken from Harvard CMT Catalog. Data for main shock is from Talebian et al. (2006). ‡ Determined by Miyake et al. (2003) method. *From IGTU: Lat.:30.711, Long.:57.188 and Depth=25.4.

4. RESULTS

From spectral ratio analysis the corner frequencies of 0.2 and 0.65 Hz have been determined respectively for the main and aftershock events (**Figs 4.1**&**4.2**). The moment ratio of 65 was estimated which gives a moment magnitude of 5.2. This is in fair agreement with the value of 5.1 reported by Harvard CMT.

In **Fig. 4.3**, we present the results of the simulations and their comparisons with the observed strong ground-motion recordings. In general, the synthetics are in good agreement with observations in almost all cases, considering inherent limitations of the method and its simplicity. **Fig. 4.4** shows the mean modelling bias for all 4 simulated records calculated as the logarithm of the ratio of the observed to simulated response spectrum. Table 4.1 represents the simulated and observed mean peak horizontal accelerations at four sites.

Table 4.1. Simulated and observed mean peak horizontal accelerations at four sites.

	ZAR	QAD	SHI	CHT
Mean observed/ Simulated (cm/s/s)	276/247	177/299	348/350	71/128

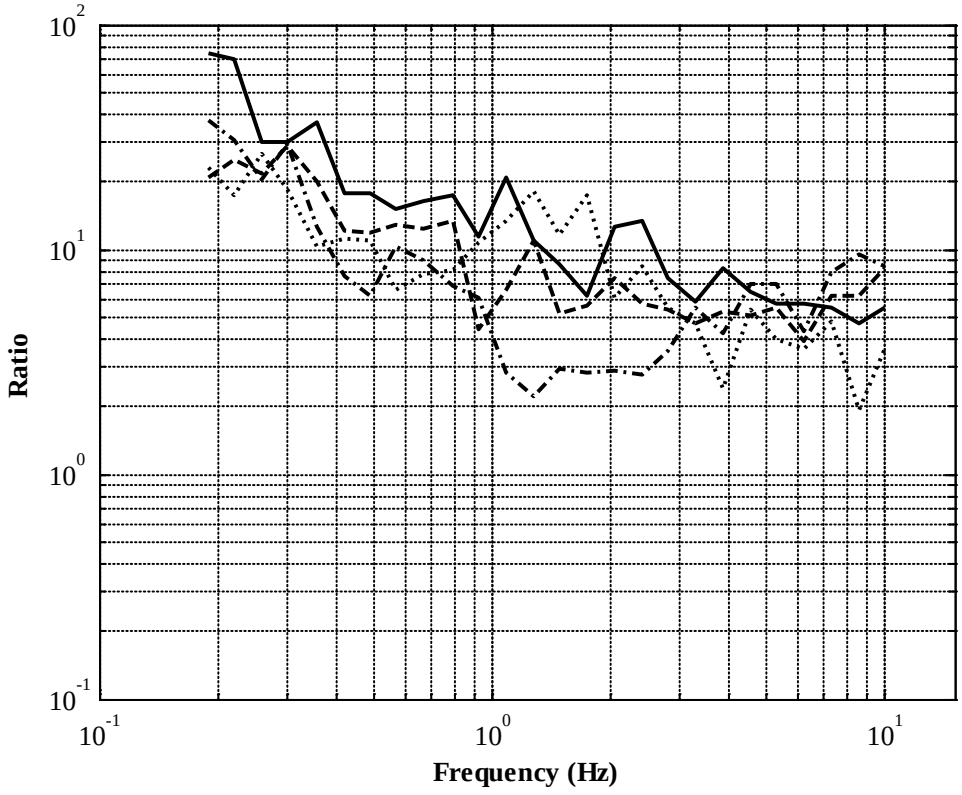

Figure 4.1. Source spectral ratios of the mainshock to four records of aftershock

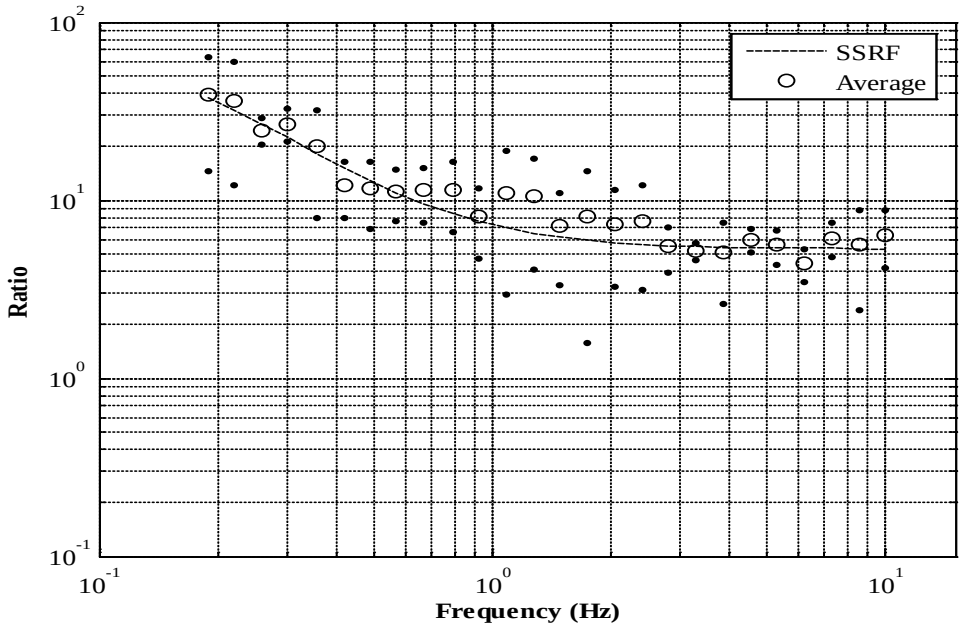

Figure 4.2. Comparison of average values of the observed ratios and best-fit source spectral ratio function (dashed line). Closed circles represent the average and bold circles give the standard deviation of the observed ratios.

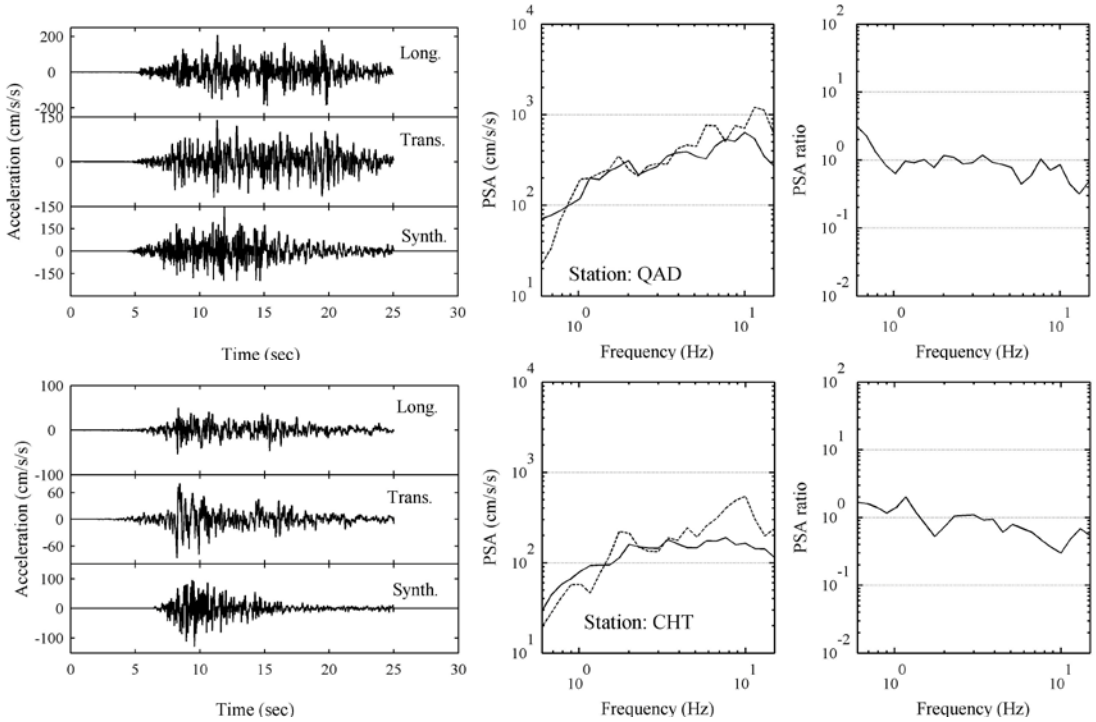

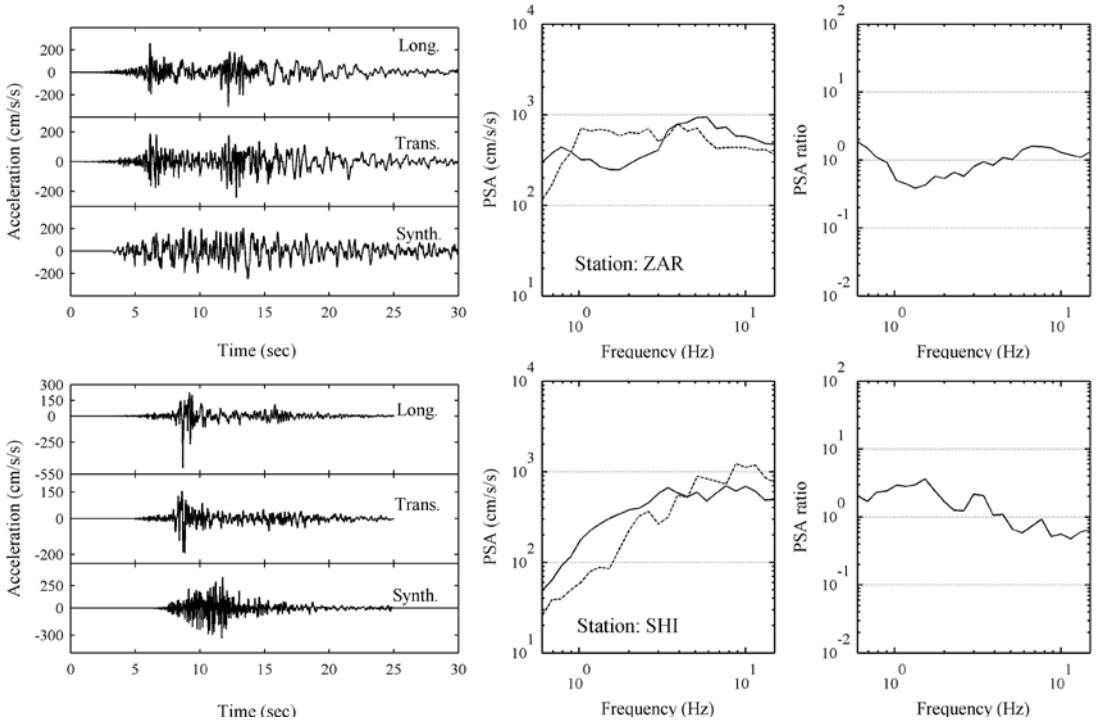

Figure 4.3. Comparison of the simulated acceleration time histories with observed records (left). The observed 5% damped pseudo-acceleration response spectra and the spectra simulated in this study are also shown (centre). The average spectra of the two horizontal components are shown by solid lines. Simulated spectra are shown by dotted lines. On the right Figure, the ratio of observed to simulated spectra is also shown.

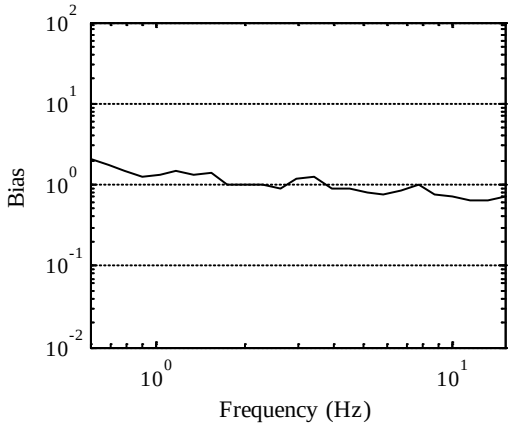

Figure 4.4. The bias calculated as the logarithm of the ratio of the observed to simulated response spectrum, averaged over all stations.

5. CONCLUSION

Two popular distinct methods of strong motion simulation, i.e. stochastic finite-faults and empirical Green's function methods have restrictions which pose limitation on the practical applications in the regions such as Iran. A new method has been proposed for simulation of strong motion based on a combination of finite-faults and empirical Green's function methods, in order to overcome the drawbacks of both methods while retaining their benefits. The generally good agreement between simulated and recorded accelerograms from the 22 February 2005 Zarand earthquake shown in this study indicates that the proposed technique has the capability of reproducing the main characteristics of strong ground motion. The method does not include the nonlinear soil response. This is not a

significant restriction/shortcoming because, Iran is a mountainous country with dry weather conditions and a low water table in most areas, and thus the nonlinear site effects are less significant.

AKCNOWLEDGEMENT

This study was supported by the International Institute of Earthquake Engineering and Seismology (IIEES) and the Iran's National Elites Foundation funds for young researchers, Project No. 9602/91"Statistical investigation of seismicity patterns before the large earthquakes in Iranian plateau, for mid-term earthquake prediction". This financial support is gratefully acknowledged. The author also, acknowledges the Building and Housing Research Center of Iran for providing them with the accelerograms used in the current study and shear wave velocity for some of the stations.

REFERENCES

Beresnev, I. A. and Atkinson, G.M. (1997) Modeling Finite-Fault Radiation from the Omega-n Spectrum, Bulletin of the Seismological Society of America, **87**, 67–84.

Beresnev, I. A. and Atkinson, G.M. (2002) Source parameters of earthquakes in eastern and western North America based on finite-fault modeling, Bulletin of the Seismological Society of America, **92**, 695–710.

Boore, D. M. (1983), Stochastic Simulation of High-frequency Ground Motions Based on Seismological Models of the Radiated Spectra, Bulletin of the Seismological Society of America, **73**, 1865–1894.

Brune, J. N. (1970). Tectonic stress and the spectra of seismic shear waves from earthquakes, J. Geophys. Res. **75**, 4997-5009.

Brune, J. N. (1971). Correction, J. Geophys. Res. **76**, 5002.

Frankel, A. (1995) Simulating strong motions of large earthquakes using records of small earthquakes: the Loma Prieta mainshock as a test case, Bulletin of the Seismological Society of America, **85**, 1144–1160.

Haddon, R. A. W. (1996) Use of Empirical Green's Functions, Spectral Ratios, and Kinematic Source Models for Simulating Ground Motion, Bulletin of the Seismological Society of America, **86**, 597–615.

Hartzell, S. (1978) Earthquake aftershocks as Green's functions, Geophysical Research Letters, **5**, 1–4.

Hartzell, S. (1992) Estimation of near-source ground motions from a teleseismically derived rupture model of the 1989 Loma Prieta, California, earthquake, Bulletin of the Seismological Society of America, **82**, 1991–2013.

Hartzell, S., Harmsen, S., Frankel, A. and Larsen, S. (1999) Calculation of broadband time histories of ground motion: Comparison of methods and validation using strong-ground motion from the 1994 Northridge earthquake, Bulletin of the Seismological Society of America, **89**, 1484–1504.

Irikura, K. (1983) Semi-Empirical Estimation of Strong Ground Motions During Large Earthquakes, Bulletin of the Disaster Prevent Research Institute, Kyoto University, **33:298**, 63-104.

Miyake, H., Iwata, T. and Irikura, K. (2003) Source Characterization for Broadband Ground-Motion Simulation: Kinematic Heterogeneous Source Model and Strong Motion Generation Area, Bulletin of the Seismological Society of America, **93**, 2531-2545.

Ordaz, M., Arboleda, J. and Singh, S. K. (1995) A scheme of random summation of an empirical Green's function to estimate ground motions from future large earthquakes, Bulletin of the Seismological Society of America, **85**, 1635 –1647.

Pavic, R., Koller, M., Bard, P. and Lacave-Lachet, C. (2000) Ground motion prediction with the empirical Green's function technique: an assessment of uncertainties and confidence level, Journal of Seismology, **4**, 59–78.

Plicka, V. and Zahradnik, J. (2002) The EGF Method for Dissimilar Focal Mechanisms: the Athens 1999 Earthquake, Tectonophysics, **359**, 81-95.

Kohrs-Sansorny, C., Courboulex, F., Bour, M. and Deschamps, A. (2005) A Two-Stage Method for Ground-Motion Simulation Using Stochastic Summation of Small Earthquakes, Bulletin of the Seismological Society of America, **84**, 31–46.

Talebian, M., Biggs, J., Bolourchi, M., Copley, A., Ghassemi, A., Ghorashi, M., Hollingsworth, J., Jackson, J., Nissen, E., Oveisi, B., Parsons, B., Priestley, K., and Saiidi, A. (2006) The Dahuiyeh (Zarand) earthquake of 2005 February 22 in central Iran: reactivation of an intramountain reverse fault, Geophysical Journal International, **164**, 137–148.